Fusion-Enabled Pluto Orbiter and Lander

Ms. Stephanie J. Thomas* and Mr. Michael A. Paluszek†
Princeton Satellite Systems, Plainsboro, NJ, 08536, US
Dr. Samuel Cohen‡
Princeton Plasma Physics Laboratory, Princeton, NJ, 08543, US

In this paper we present the results of our NIAC Phase I Study on a Fusion-Enabled Pluto Orbiter and Lander. The enabling technology, Direct Fusion Drive, is a unique fusion engine concept based on the Princeton Field-Reversed Configuration (PFRC) fusion reactor under development at the Princeton Plasma Physics Laboratory. The truly game-changing levels of thrust and power in a modestly sized package could integrate with our current launch infrastructure while radically expanding the science capability of these missions. NIAC grants require that a technology be studied in the context of a specific mission. Our mission context is the delivery of a Pluto orbiter with a lander, which cannot be done with any other technology. Direct Fusion Drive (DFD) provides moderate thrust to allow for reasonable transit times to Pluto while delivering substantial mass to orbit: 1000 kg delivered in four years using 5 N constant thrust. Since DFD provides power as well as propulsion in one integrated device,[1] it will also provide as much as 1 MW of useful electrical power to the payloads upon arrival. This enables high-bandwidth optical communication, powering of the lander from orbit, and radically expanded options for instrument design.

I. Introduction

Figure 1 shows an artist's rendering of a DFD engine. This notional engine has eight field shaping coils, two smaller mirror coils, and two additional nozzle shaping coils. Note the relatively thin shielding shown inside the magnets; this is necessary to protect the superconductors from the small amount of neutron radiation the engine will produce. Coolant lines running through the shielding will collect thermal energy from the neutrons, bremsstahlung radiation, and synchrotron radiation. A small neutral beam injects the fusion fuel into the center of the engine, while propellant enters from the ionizing gas box on the righthand side. The mass of the engine is dominated by the magnet coils and the shielding, as the graphic indicates.

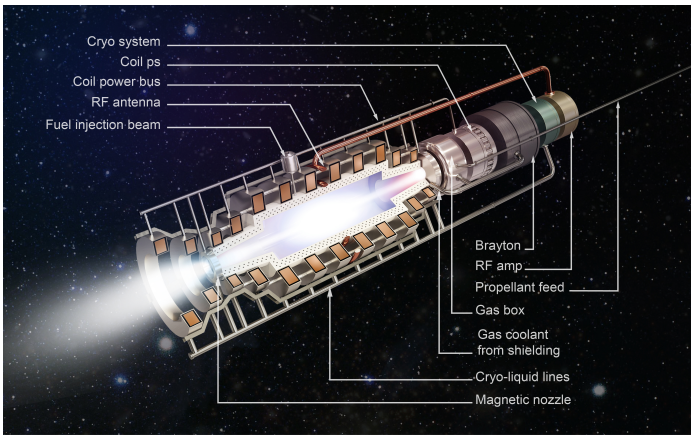

Figure 1. Artist's Rendering of the Direct Fusion Drive, based on the Princeton Field-Reversed Configuration fusion reactor

This paper will first review the technology underlying the DFD, the Princeton Field-Reversed Configuration (PFRC), which is a steady-state fusion reactor concept with heating via rotating magnetic fields. A thrust model of the reactor is presented that is based on a fluid code modeling the exchange of energy in the plasma surrounding the reactor. We will review the Pluto mission architecture based on this engine model including the departure from low-Earth

*Vice President, AIAA Senior Member.
†President
‡Job Title, Department, Address.

orbit, the transfer to Pluto, and the insertion to Pluto orbit. The goal of the Pluto mission is to deliver a 1000 kg payload to Pluto as soon as possible using a direct trajectory, with no planetary swingbys. Finally, we present initial design work on the engine and vehicle, including the superconducting coils, shielding, power conversion system, radiators, and structural analysis. We conclude that the mission is feasible if an engine specific power of between 750 and 1250 W/kg can be achieved.

II. PFRC and DFD

The Direct Fusion Drive concept is an extension of ongoing fusion research at Princeton Plasma Physics Laboratory dating to 2002.[2–5] The Princeton Field-Reversed Configuration machine (PFRC) employs a unique radio frequency (RF) plasma heating method invented by Dr. Samuel Cohen. Odd-parity heating was first theorized in 2000[6] and demonstrated in the 4 cm radius PFRC-1 experiment in 2006.[7] Experiments are ongoing with the second-generation machine, PFRC-2, which has a plasma radius of 8 cm (Figure 2). Studies of electron heating in PFRC-2 have surpassed theoretical predictions, recently reaching 500 eV with pulse lengths of 300 ms, and experiments to measure ion heating with input power up to 200 kW are ongoing. When scaled up to achieve fusion parameters, PFRC would result in a 4-8 m long, 1.5 m diameter reactor producing 1 to 10 MW. This reactor would be uniquely small and clean among all fusion reactor concepts, producing remarkably low levels of damaging neutrons.

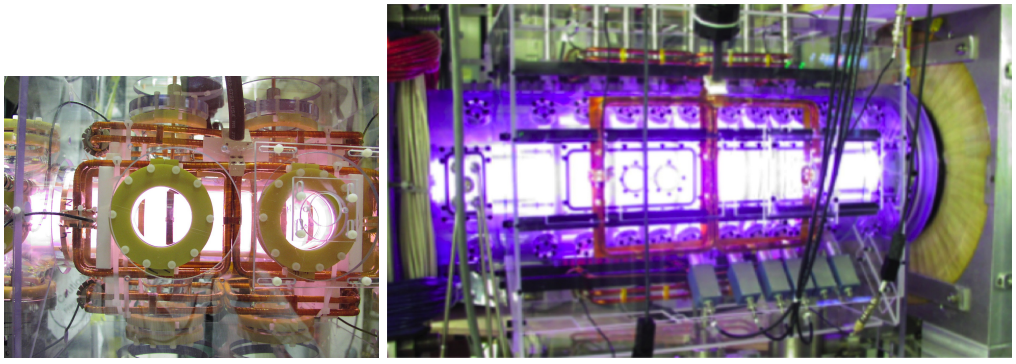

Figure 2. PFRC-1 and PFRC-2 Experiments. The RF antenna are visible wrapped in orange Kapton tape.

The plasma heating method uses a unique configuration of the radio antenna. Attempts have been made to heat FRC plasmas with RF before, but always with single-loop antenna that resulted in a near-FRC plasma but with open field lines. We call this even-parity heating due to the symmetry of the induced magnetic field. Open field lines give the plasma an opportunity to escape and reduce confinement time. In contrast, the PFRC antenna are figure-8s. Two pairs operate 90 degrees out of phase on adjacent sides of the plasma. An antenna (wrapped in orange Kapton tape) is clearly visible on the side of PFRC-2 in Figure 2. This results in so-called odd-parity heating - the magnetic field on one side of each figure-8 is in the opposite direction as the other side - and closed field lines in the generated FRC. Closed field lines keep the plasma trapped as it is heated. The oscillation of the currents in the RF antenna result in a rotating magnetic field, RMF, with about 0.3% of the strength of the axial magnetic field.

Reduction in neutrons is achieved through multiple channels. First and foremost, our choice of Helium-3 (^{3}He) and deuterium (D) fuels results an an aneutronic primary reaction. However, there are still D-D side reactions, the proportion of which is governed by the fusion cross-section at the relevant ion temperature. The D-D side reactions are divided equally into two, a D-D reaction producing a 2.45 MeV neutron and a D-D reaction producing tritium (T). This tritium can then fuse with deuterium to produce a high energy 14.7 MeV neutron.

$$\mathrm{D} + {}^3\mathrm{He} \rightarrow {}^4\mathrm{He}\ (3.6\ \mathrm{MeV}) + \mathrm{p}\ (14.7\ \mathrm{MeV}) \quad (1)$$

$$\mathrm{D} + \mathrm{D} \rightarrow \mathrm{T}\ (1.01\ \mathrm{MeV}) + \mathrm{H}\ (3.02\ \mathrm{MeV}) \quad (2)$$

$$\mathrm{D} + \mathrm{D} \rightarrow {}^3\mathrm{He}\ (0.82\ \mathrm{MeV}) + \mathrm{n}\ (2.45\ \mathrm{MeV}) \quad (3)$$

The PFRC is specifically designed to produced the absolute minimum number of neutrons from these side reactions. One, the small size of the reactor results in a favorable ratio of surface area to plasma volume,

reducing the wall load compared to larger machines. Two, we adjust the operating fuel ratio of ^{3}He:D to 3:1, sacrificing some power density for lower radiation. Three, the reactor is designed to rapidly eliminate the tritium produced by the D-D side reactions, preventing any D-T reactions from occurring. This means that the only neutrons produced are those with energy of 2.45 MeV. A fourth reduction in neutrons may occur due to preferential heating of the ^{3}He over the D by the rotating magnetic fields; at the correct frequency, we estimate that the ^{3}He may reach a temperature of 140 keV while the D is only at 70 keV. This would result in another (CHECK) 10 fold reduction in neutrons. The final result of these design features is that only 1%, or perhaps even only 0.5% or less, of the fusion power is in 2.45 MeV neutrons, and the power in 14.7 MeV neutrons is effectively zero.

The tritium is eliminated due to its interaction with the cool scrape-off-layer (SOL) surrounding the fusion region. The size of the reactor is such that the ratio of the tritium gyroradius to the scrape-off-layer radius, the s factor in plasma physics terminology, is low - about 2.3. This forces the tritium to pass through the SOL repeatedly. When the tritium particles pass through the cool SOL plasma, electron drag causes energy to be transferred from the tritium to the SOL electrons. When this has happened a few times, the tritium is captured by the SOL field lines and flows out the open end of the reactor. The burn-up time for energetic tritium to fuse is about 20 seconds, while the time in which it will cool and be trapped in the SOL is just 20 ms. The same process occurs for the other fusion ash products, which are all effectively exhausted.

Parameter	**DFD**
Fuel	D-^{3}He
r_s	0.3 m
Elongation, κ	5
B_{axial}	4.3 T
B_{nozzle}	20 T
β	0.84
^{3}He:D	3
n_e	3 $\times 10^{20}$ m^{-3}
T_e	30 keV
T_i	100 keV
S*/κ	2.8
γ_{LH}	0.02
s_{T+}	2.3
s_{fuel}	10

Figure 3. Parameters for a 2-MW engine

Figure 3 gives parameters for a 2 MW engine design point. Two stability criteria for fusion reactors are given: the lower-hybrid micro-stability ratio, γ_{LH}, at 0.02 is $\ll 1$; and the macro-stability criterion, S*/κ, is less than 3. The lower-hybrid drift instability would produce unwanted turbulence reducing the effectiveness of heating. The low value of the macro-stability criterion shows that the PFRC plasma is kinetic rather than fluid-like, with low collisionality. This means the PFRC is not subject to the tilt instabilities predicted by MHD theory for larger machines.

The PFRC is perfectly suited for use as an engine for two reasons: one, the configuration results in a tremendous reduction of neutron production compared to other D-^{3}He approaches as detailed above; two, the directed axial flow of cool SOL plasma which absorbs the energy of the fusion products. When the divertor end of the PFRC is configured with a magnetic nozzle, the reactor becomes the Direct Fusion Drive (DFD). Adding additional propellant to the SOL flow results in a moderate thrust, high specific impulse exhaust stream. We call this process *thrust augmentation* of the reactor, shown in Figure 4.

The low neutron production is crucial to minimizing the shielding required in space and hence maximizing the engine specific power. We estimate that 10 cm of boron-carbide shielding will be sufficient for a medium-duration mission; this ceramic material will also provide structural support and house the coolant channels for the thermal conversion cycle.

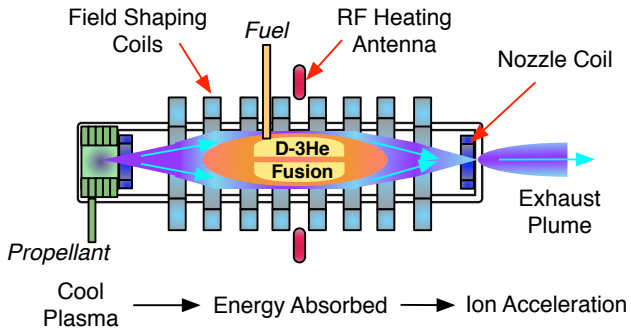

Figure 4. DFD Schematic. Cool plasma flows around the fusion region, absorbs energy from the fusion products, and is then accelerated by a magnetic nozzle.

III. DFD Thrust Model

The cool plasma in the scrape-off-layer, less than 100 eV, is in a regime suitable for fluid analysis. UEDGE is a 2-D multi-species fluid code that predicts electron and ion temperatures based on a specified magnetic configuration and plasma, neutral gas, and power input. Lawrence Livermore National Lab staff wrote and maintain this code.[8] Figure 5 shows the UEDGE field geometry for studying the PFRC scrape-off-layer; note the length along the major axis of about 10 m while the radius is only 0.4 m. Along the length, the gas box where propellant is ionized is 1-m long on the far left, electron heating occurs in the central 2 m, and the magnetic nozzle is located at $z \approx 2$ m.

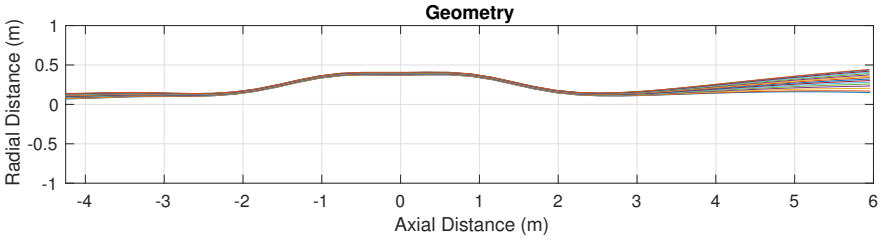

Figure 5. UEDGE Field Geometry

PPPL has generated UEDGE data for a large data set of input powers and flow rates using this geometry. Figure 6 shows example data from a single UEDGE run, with an input power of 0.5 MW and a gas flow of 0.05 g/s. The electron temperature is highest in the 2 m core section. Note the increase in the ion kinetic energy in the plume, past the magnetic nozzle, with an exit energy of 70 eV.

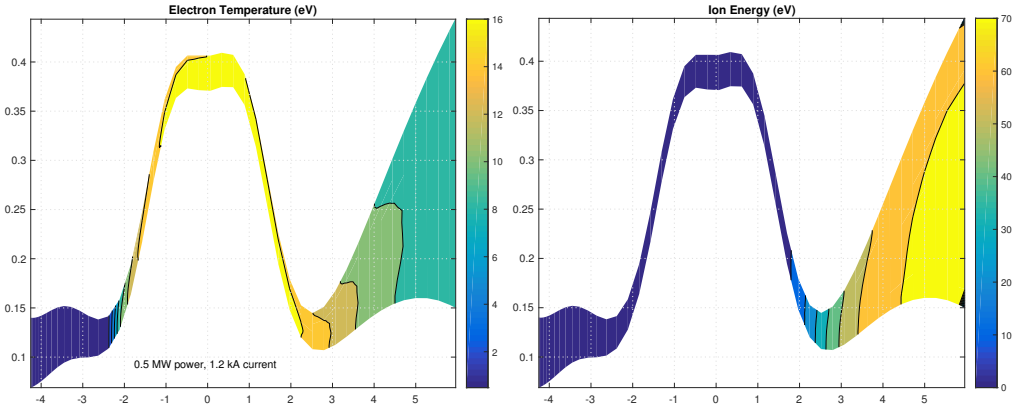

Figure 6. UEDGE Thrust Data and Model

Figure 7 shows resulting thrust data from a large set of UEDGE runs on the left. The gas flow rate varies from 0.02 to over 0.7 g/s. The legend shows the input power, which is the power transferred to the SOL electrons from the fusion ash products and NOT the total fusion power, which would be higher. The region of operation we want is the nearly linear section for each power level before the thrust starts to drop off. Black markers indicate the desired region along each line. At higher flow rates for a given power level, the electrons can no longer absorb all the power and some power goes directly to the wall, resulting in the loss of thrust.

A numerical fit to the data was obtained by treating the operating region as a linear function of flow rate, and separately solving for the slope and intercept of these lines as a function of input power. The results of these linear fits are shown in Figure 8. A second order polynomial was used for the slope of the thrust lines and a first order polynomial for the intercept. Exhaust velocity is easily converted to thrust using $T = u_E \dot{m}$, i.e. multiplying by the flow rate, so we can use either fit for our functional model. This function can then be used to compute an estimated thrust for any chosen combination of flow rate and (SOL) input power. We found that using the thrust fit coefficients led to less total error in both the estimated thrust and exhaust velocity at all power levels and flow rates.

Figure 9 shows the results of the model for a continuous range of power and flow. We have applied limits on the allowable flow rate.

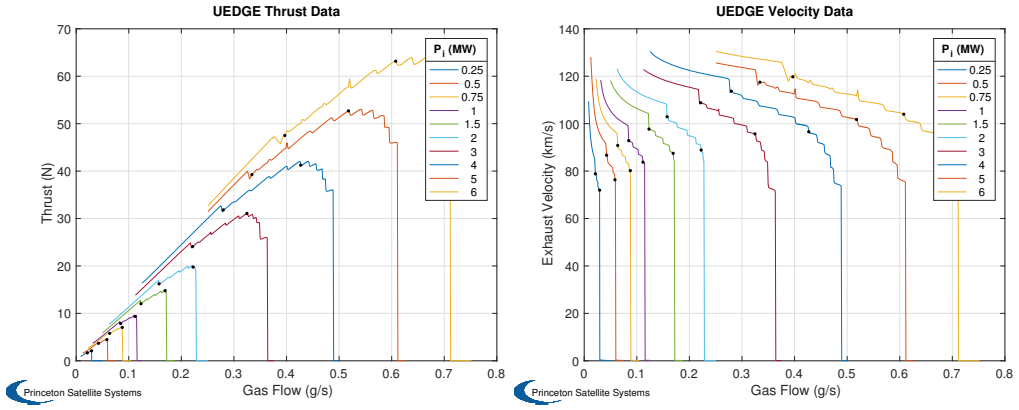

Figure 7. UEDGE Thrust and Velocity Data

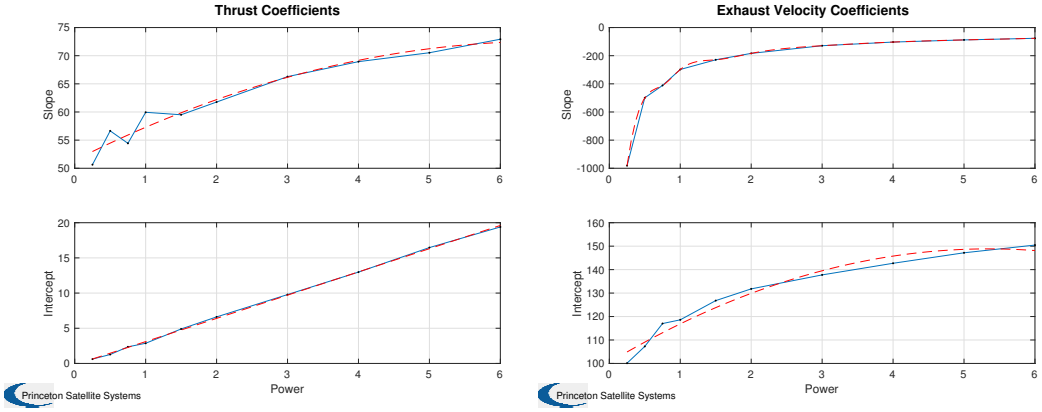

Figure 8. UEDGE Velocity Data and Model

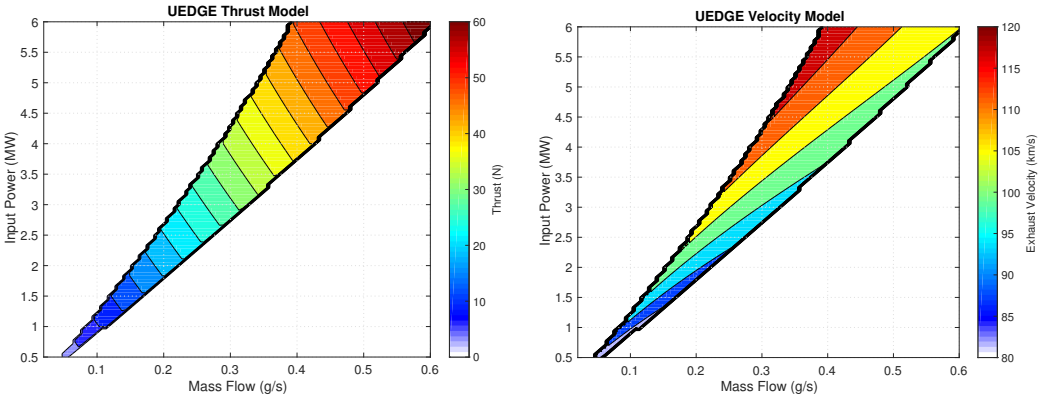

Figure 9. Thrust and Velocity Model

IV. Pluto Mission Architecture

For our NIAC analysis, we looked at the transfer to Pluto as well as both Earth departure and Pluto arrival spirals. Initial analysis of the Pluto mission relied on simple Lambert trajectories that assumed relatively short acceleration and deceleration phases at the beginning and end of the trajectory. The power level is an input, along with a specific power and thrust efficiency, which then determines the Isp given a thrust level. This simple analysis indicated that assuming a fairly conservative specific power of 0.7 kW/kg, a mission was possible under 8000 kg using two 1 MW engines. This would fit on a single Delta IV Heavy launch. The mission would deliver 1000 kg to Pluto and then provide about 1 MW of electrical power on orbit. Figure 10 shows the mission parameters assuming a 74 km/s transfer, which is possible for a launch date in 2036. A burn time of 292 days corresponds to a required thrust of 16.2 N and an Isp of 12,554 seconds, assuming an overall thrust efficiency of 0.5.

Payload	1000 kg
Fusion Power	2 MW
Total Trip Time	4 years
Acceleration Time	292 days
Specific Power	0.7 kW/kg
Thrust Efficiency	0.5
Total ΔV	74 km/s
Thrust	16.2 N
Isp	12,554 s
Total Mass	7158.7 kg
Engine Mass	2857.1 kg
Fuel Mass	3236.9 kg
Quantity ^{3}He	0.4 kg

Figure 10. Point Mission Design using Lambert Trajectory

Our thrust analysis from the previous section indicates that a reasonable thrust level ranges from 5 to 10 N per MW of SOL input power. Keeping in mind that the power into the SOL is some fraction of the total fusion power, perhaps 50%, that corresponds to a range of 2.5 to 5 N per MW of fusion power. This would mean that our trajectories should be limited to 5 N of thrust for a single 1 MW engine and 10 N of thrust for two. UEDGE is not necessarily capturing the full efficiency of the magnetic nozzle, nor is the field configuration optimized for producing thrust, so it is possible that performance could be higher, but this is a good benchmark. Further numerical studies with variable magnetic geometry, which can include more of the nozzle region, are ongoing.

We wrote a direct method optimization to reach a planar target in a fixed amount of time with constant thrust and minimum mass. The mass is the combination of the fuel mass, engine mass, payload mass, and accounts for a fuel tankage fraction. The inputs are the specific power, initial and final radii, exhaust velocity, and thrust efficiency. There are a fixed number of points along the trajectory, and the degrees of freedom are the thrust angle at those discrete points. In MATLAB, this is solved using the `fmincon` function in the Optimization Toolbox. Figure 11 shows an example trajectory generated this way, which shows that the orbit follows a good portion of the Earth's orbit before it peels away in the direction of Pluto. From thereafter, it resembles the straight-line trajectory. This is accomplished with a thrust of just 4 N and a power of 0.5 MW, requiring a fuel mass of 5001.41 kg and a total mass of 6746.75 kg.

Figure 11. Planar Pluto Trajectory

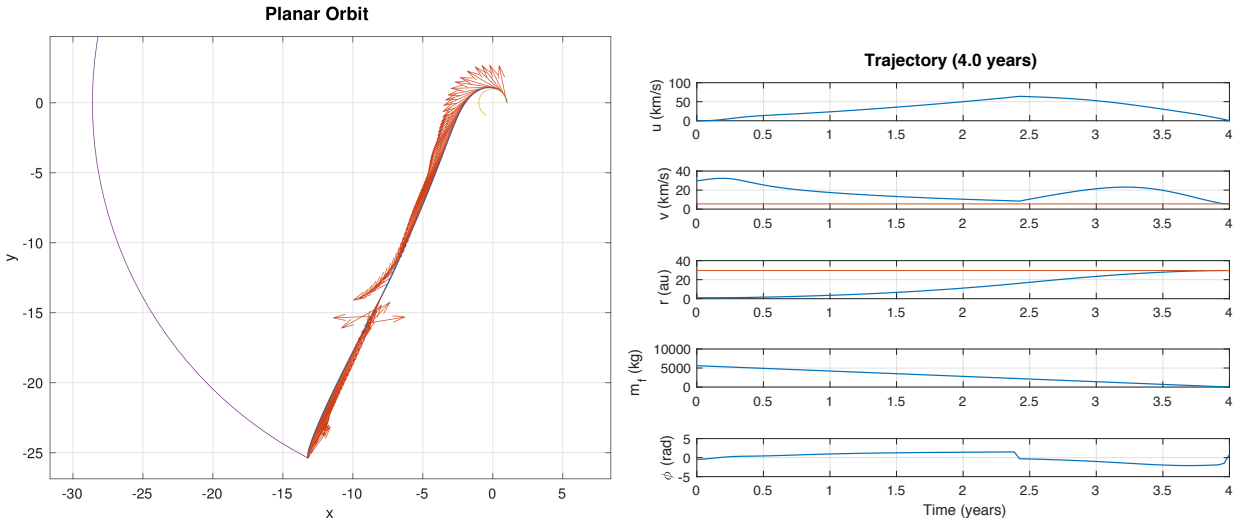

Figure 11 shows the time history plots of the radial velocity u, tangential velocity v, radius r (in astronomical units), fuel mass m_f, and thrust angle ϕ. The tangential velocity initially increases, and then begins decreasing after about 0.2 years. The parameters for this example are 1000 kg payload, 4-year duration,

exhaust velocity of 100 km/s, thrust efficiency of 0.4, a specific power of 1000 W/kg, and a fuel structural fraction of 0.05. The total delta-V applied is 135.21 km/s. (The final distance of Pluto orbit is 29.60 AU).

Since the trajectory is very nearly a straight line, we can use a much simpler 1-D straight-line analysis to more easily compare different mission durations, payload masses, and resulting mission mass and required thrust. The switch time from acceleration to deceleration can be calculated directly in this case. This is also an optimization using `fmincon` but now there is just a single variable, the thrust. To deliver 1000 kg in 4 years with the same parameters as the previous planar solution, the straight-line solution returns 4.57 N thrust using 0.57 MW power, the fuel mass is 5770.47 kg and the total mass is 7630.41 kg.

Figure 12. Straight-Line Pluto Trajectory

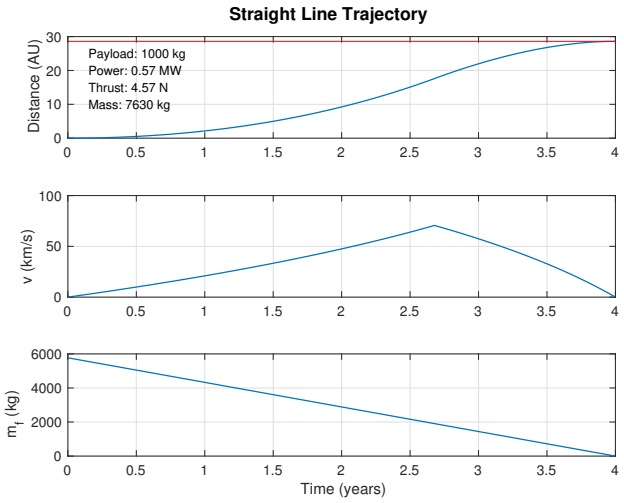

The original departure concept in our NIAC proposal was to insert the Pluto spacecraft directly into heliocentric orbit. This required a Delta IV Heavy class booster, which can deliver a maximum of 8000 kg to MTO. Analysis shows that an Earth departure from LEO uses very little fuel and takes between 25 and 60 days depending on engine parameters and vehicle mass. This allows a launch by almost any launch vehicle, dramatically reducing launch and overall mission costs while increasing the allowable mission mass. For example, a Falcon 9 can deliver 13150 kg to LEO. It also allows checkout and testing in low Earth orbit. A sample departure spiral is shown on the left in Figure 13 for a thrust of 10 N, exhaust velocity of 100 km/s, and initial mass of 7500 kg. The red disk is the inner Van Allen belt. As can be seen, little time is spent there. The total time in the belt for this case is 14.37 days. The outer belt is not a source of radiation damage. The delta-V for the spiral is about 7 km/s.

We wrote a 2D optimization to study the Pluto insertion from a hyperbolic approach with a fixed thrust and mass. The question to answer is, will it be possible to insert into orbit using the relatively low thrust of 5-10 N, and how much time and delta-V should be allocated. Our study has indicated that insertion will require less than 1 km/s delta-V, which is a small portion of the mission total. It is easily accomplished in about one day with 20-40 N thrust and in 2-3 days with 10 N thrust, as shown on the right in Figure 13.

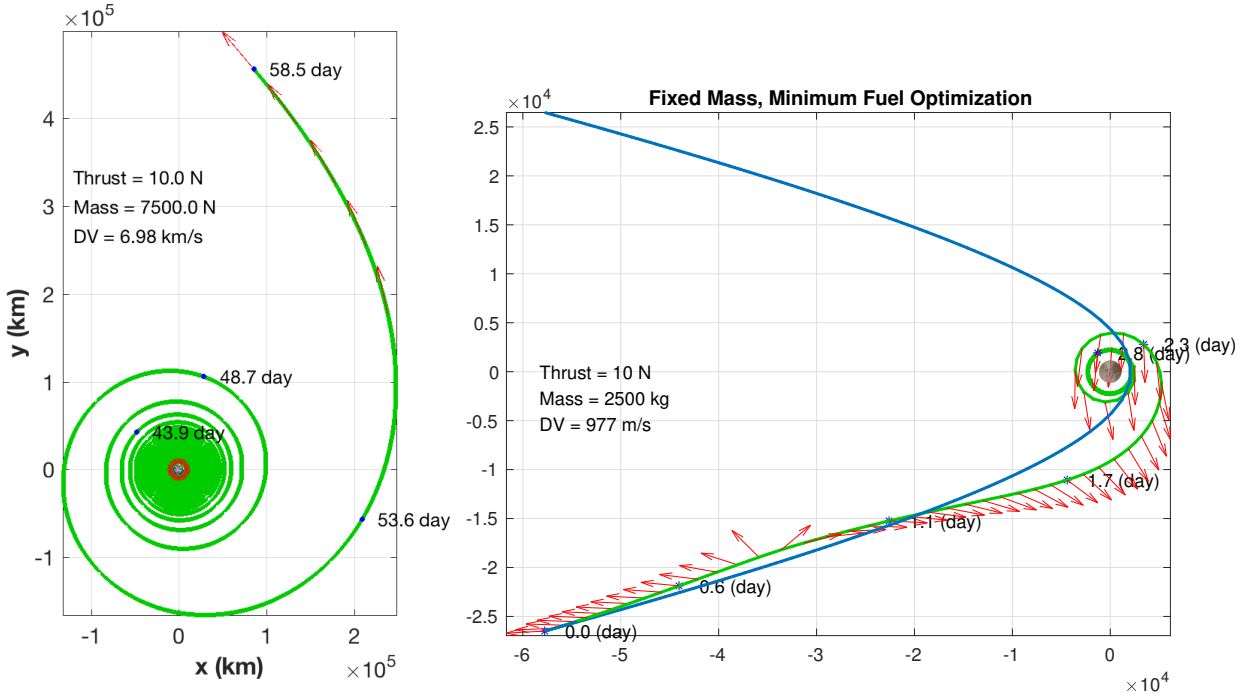

Figure 13. Earth and Pluto Spirals for 10 N Thrust

V. Engine and Vehicle Design

Our NIAC project included analysis of the following subsystems: the superconducting coils, heat extraction system, startup system, radiators, and shielding, see Figure 14. Note that the reactor is small enough that it can be started up in space using a combustion auxilary power unit using just a few kilograms of stored oxygen. We developed a parametric engine model from this analysis that allows us to size an engine anywhere in the range of 1 to 10 MW, and estimate its specific power. We created a nominal vehicle design from this model by sizing the engines, the fuel tanks, and the radiators for the Pluto mission.

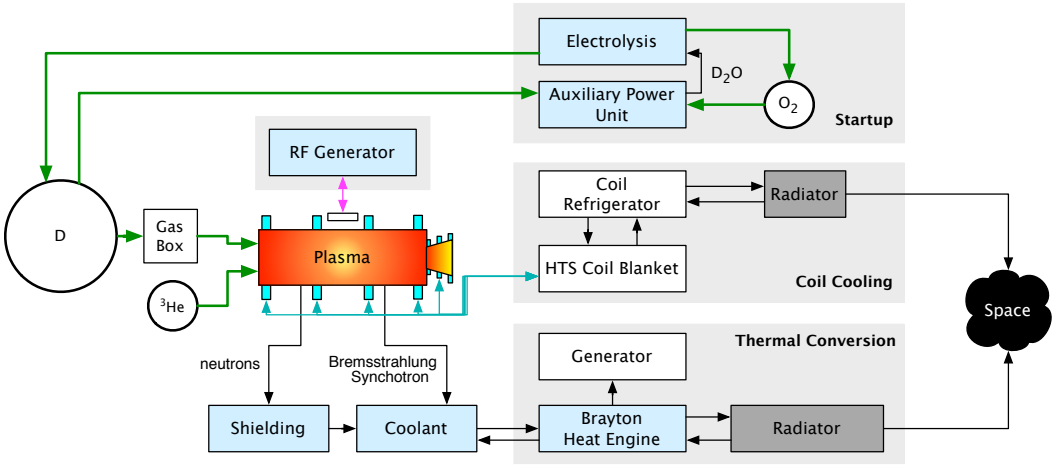

Figure 14. Subsystems Block Diagram

V.A. Vehicle Design

The vehicle and lander design concepts are shown in Figure 16 with two 1 MW engines. The vehicle has optical lasers for communication on trusses. There are small solar panels for Earth orbit checkout. The long

dark wings are the space radiators. In sizing the tanks, we assume that the deuterium will be stored as a liquid while the Helium-3 can be stored as a gass, since there is such a small quantity. The orbiter will beam about 50 kW of power to the lander using a specially tuned laser. The lander solar array is on a small truss to allow it to track the orbiter for receiving the optically transferred power. The lander is allocated 230 kg of the 1000 kg total payload mass.

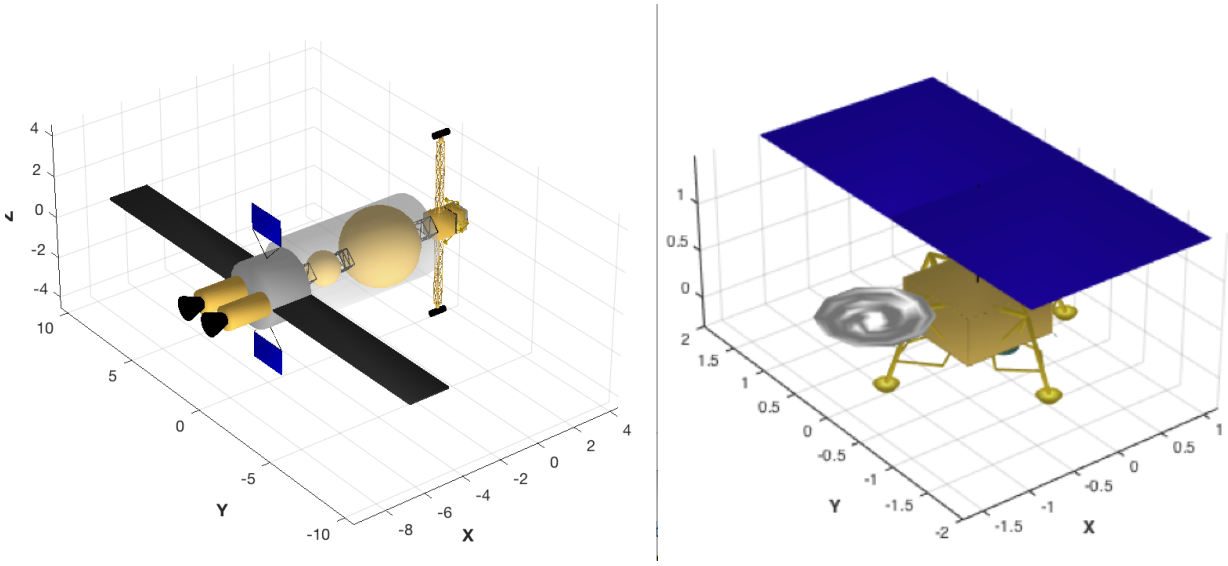

Figure 15. Vehicle and lander models as represented in MATLAB using the Spacecraft Control Toolbox

Figure 16 shows the mass breakdown for the reference vehicle. An engine specific power of 0.7 was used. The entire non-thrust power of 840 kW was allocated to the radiators for sizing. After allowing for the radiators and lander, there is 636.5 kg left for the rest of the orbiter vehicle.

Component	Mass
Deuterium	3364 kg
Helium-3	0.4 kg
Lander	230 kg
Orbiter	636.5 kg
Radiators	133.5 kg
Fuel Tanks	368.25 kg
Propulsion	2857 kg
TOTAL MASS	7724 kg

Component	Dimension
Deuterium Tank Radius	1.8 m
Helium-3 Tank Radius	0.95 m
Radiator Wing Length	12 m
Engine Length	4 m

Figure 16. Vehicle Mass and Sizing Parameters

Current space-qualified radiators will be too heavy but there are upcoming radiator materials that will make the radiators mass a small fraction of the engine total. NASA is currently supporting research in this area, such as the work on carbon-carbon radiators performed by the University of Massachusetts with the support of the MSFC Center Innovation Fund.[9] The goal is to reduce the areal mass of radiators from about 10 kg/m^2 currently to 2 kg/m^2 or less. Our current work assumes carbon-carbon radiators with an areal mass of 2.75 kg/m^2 and an average temperature of 625 K. As a point example, assume the radiators need to dissipate 500 kW. Recall that the black body radiation equation is $Q = A\epsilon\sigma T^4$. Assume the radiator emissivity is 1, then the total area required to radiate 500 kW at 625 K is 57.8 m^2, or taking into account both the front and back radiator surfaces, a total radiator size of 28.9 m^2. If there are two wings then each might be 2 m by 7.2 m. With an areal mass of 2.75 kg/m^2 then both wings together would have a mass of 79.5 kg. For comparison, consider a traditional system with an emissivity of 0.8, areal mass of 10 kg/m2, and a maximum temperature of 400 K. The total area would now be 215.3 m^2 and the mass 2153 kg!

We also assume that the cryogenic deuterium fuel tank will be made of composites. NASA has been funding work on such tanks, and testing a 2.4 meter diameter tank made by Boeing in 2013 and a larger 5.5-

meter tank in 2014.[a] The tank is now considered TRL 6, and this size is already adequate for our application. The NASA study compared state-of-the-art metallic tanks to the composite tanks for a standard 10 m tank diameter, sufficient for SLS. The metallic tank, at a mass of 11,000 lbs, holding 81556 lbs of liquid hydrogen, would have structural fraction about 13%, while the composite tank weighing only 6700 lb would have a fraction about 8%. The highly optimized metallic shuttle external tanks have an overall structural fraction of about 3.5%, with the LH2 tank alone having a fraction of about 12.7%[b]. Therefore, for our trajectory sizing calculations, an optimistic structural ratio of 0.05 is used.

V.B. Engine Design

Figure 17 gives a power flow diagram for a 1 MW engine. Approximately 45% of the fusion power goes to thrust, 20% to bus electric power, 20% lost to heat, and 10% is recirculated for the RF heating. This is determined by modeling the power generated per volume by the reactor, and the power lost to synchrotron, bremsstrahlung, and neutrons. We must then estimate the conversion efficiency from the heat to electricity, which is up to 60% for a Brayton cycle. Though Bremsstrahlung losses may also be calculated accurately, this is not the case for synchrotron losses because of plasma absorption and wall reflections. Our model assumes full emission from a 3-cm thick shell just inside the separatrix and no wall reflection.

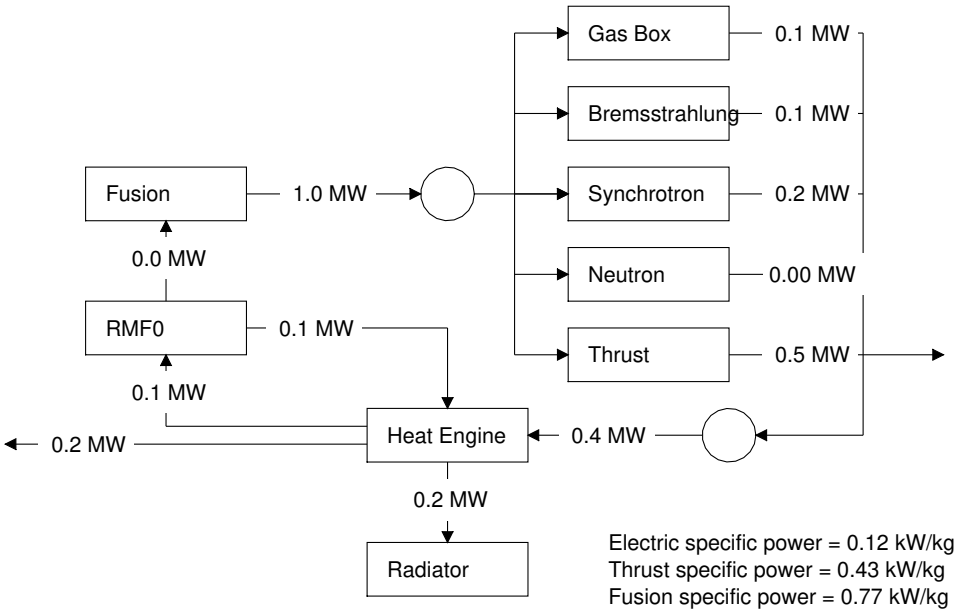

Figure 17. Power Flow for 1 MW Engine

The superconducting coils are a major portion of the engine mass. In order to estimate this mass, we reviewed published data on both low-temperature and high-temperature superconductors. For example, current generation Amperium 12 mm high-temperature wire has a current capacity of 350 A at 77 K, but 700 A at 30 K. This wire has a linear density of 0.2 g/cm. We can count the number of turns to produce 3 MA (3e6 A) in a 0.5 m radius coil: 8572 turns at 77 K and 4286 turns at 30 K, or 579 kg and 298.5 kg, respectively. Considering a single engine will require 6 to 8 such coils plus the nozzle shaping coils, producing a 1 MW engine on the order of 1000 kg is clearly driven by superconductor mass. High-temperature superconductor companies are working to make thinner tapes with less cladding, but also consider low-temperature superconductors. They need to be cooled to 4.2 K, limiting the choice of coolant and increasing cryostat mass, however, a 1.04 mm NbTi wire has a linear density of just 0.063 g/cm and a capacity of 700 A. The same number of turns of this wire would has a mass of only 84.6 kg. This huge range in avaiable properties is one reason we are continuing to pursue superconductor design in our NIAC Phase II grant and an ongoing NASA STTR.

In order to have a functional model of the coil size, we used average properties of 500 A capacity and 0.085 g/cm linear density. The necessary magnet current is determined from the input β (ratio of plasma pressure

[a]NASA Press Release 14-232, August 26, 2014
[b]https://science.ksc.nasa.gov/shuttle/technology/sts-newsref/et.html

to magnetic field) and plasma properties (temperature and density). For a typical 1 MW engine with a 0.25 m plasma radius, elongation of 5, and electron density of 3.83e+20, the estimated magnet mass with these superconductor properties is 557.25 kg and the specific power (total fusion power to total mass) is 0.77. If we instead consider a best case scenario of NbTi 0.7 mm wire with 350 A current and just 0.0372 g/cm density, the magnets would be only 354.29 kg and the specific power increases to 0.93. The less optimistic coil mass is included in the mass budget table below. The radiator mass included in these specific power estimates is just that to dissipate the thermal conversion system waste heat (0.17 MW).

Mass Budget for 1 MW Engine

Shielding	286.10 kg
Magnets	557.25 kg
Coil Cooling	17.24 kg
RMF System	107.62 kg
Power Generation	172.42 kg
Radiators	20.93 kg
Structure	150.23 kg
TOTAL MASS	1277.73 kg

Power Budget for 1 MW Engine

Gas Box	0.10 MW
Neutrons	2.27 kW
Synchrotron Radiation	0.19 MW
Bremsstrahlung Radiation	0.15 MW
Thrust Input Power	0.55 MW
TOTAL FUSION POWER	0.98 MW
Bus Power	0.15 MW
RMF Power	0.11 MW
Radiated Power	0.17 MW
TOTAL THERMAL POWER	0.43 MW

VI. Conclusion

Our Phase I NIAC analysis confirmed that our Pluto mission concept is plausible. Critical subsystems include the superconducting coils, space radiators, cryogenic systems, high-power optical transmission systems, and thermal conversion. Available data suggests that research in all these areas has made tremendous progress recently and we have not identified any roadblocks.

We received a Phase II NIAC grant in May, 2017 to continue this work, and also two NASA STTRs relating specifically to the RF subsystem and superconducting coil subsystem. We will be further refining our models and designs to create a roadmap for building the first DFD prototype. Ongoing work at PPPL on proving ion heating using the RMFo method in PFRC-2 will need to be followed by a larger machine with superconducting coils that can heat the plasma sufficiently to demonstrate fusion. We are actively searching for funding mechanisms to continue this research.

A compact 1 MW space power plant would be truly game-changing for multiple applications. In Earth orbit, it enables high-power payloads like radar as well as nearly unlimited orbit maneuverability. In cislunar space, DFD could transform the envisioned Deep Space Gateway while also powering human bases on the lunar surface. Robotic missions to asteroids, Jupiter and its moons, and any other deep space destination become more faster, cheaper, and can return orders of magnitude more science. There are many missions that can be accomplished now with a small amount of helium-3 from terrestrial sources, and enormous reserves are available on the moon for future missions.

References

[1]S. Thomas, M. Paluszek, S. C., "Direct Fusion Drive: Game-changing power and propulsion in space," *Proc. 20th Conference on Advanced Space Propulsion*, Glenn Research Center, November 2014.

[2]Cohen, S., "Method To Reduce Neutron Production in Small Clean Fusion Reactors," Patent Pending, March 2012, Publication Number 20150294742.

[3]Cohen, S., Pajer, G., Paluszek, M. A., and Razin, Y., "Method And Apparatus To Produce High Specific Impulse and Moderate Thrust From a Fusion-Powered Rocket Engine," Patent Pending, May 2012, Publication Number 20150098543.

[4]Cohen, S., Stotler, D., and Buttolph, M., "Fueling Method for Small, Steady-State, Aneutronic FRC Fusion Reactors," Patent Pending, September 2013, Publication Number 20150228369.

[5]Paluszek, M., Ham, E., Cohen, S., and Razin, Y., "In Space Startup Method for Nuclear Fusion Rocket Engines," Patent Pending, August 2013, Publication Number 20150055740.

[6]Cohen, S. A. and Milroy, R. D., "Maintaining the closed magnetic-field-line topology of a field-reversed configuration with the addition of static transverse magnetic fields," *Physics of Plasmas*, Vol. 7, No. 6, June 2000.

[7]Cohen, S. A., Berlinger, B., Brunkhorst, C., Brooks, A., Ferarro, N., Lundberg, D., Roach, A., and Glasser, A., "Formation of Collisionless High-β Plasmas by Odd-Parity Rotating Magnetic Fields," *Physical Review Letters*, Vol. 98, 2007, pp. 145002.

[8]Rognlien, T., Rensink, M., , and Smith, G. R., "Users' Manual for the UEDGE Edge-Plasma Transport code," available online, 2000.

[9]Hyers, R., Tomboulian, B., Craven, P., and Rogers, J., "Lightweight, High-Temperature Radiator for Space Propulsion," online presentation, 2012.

[10]Cohen, S., C.Swanson, and McGreivy, N., "Direct Fusion Drive for Interstellar Exploration," *submitted to JBIS*, July 2017.

[11]Razin, Y. S., Pajer, G., Breton, M., Ham, E., Mueller, J., Paluszek, M., Glasser, A. H., and Cohen, S. A., "A direct fusion drive for rocket propulsion," *Acta Astronautica*, , No. 1, December 2014, pp. 145–155.